Mechanobiology of Fibroblast Activation in Skin Grafting

Yuan Hong[1,2,*], Xiangjun Peng[1,3,*], Haomin Yu[1,2,*], Mohammad Jafari[1,4], Delaram Shakiba[1,5], Yuxuan Huang[1,2], Chengqing Qu[1,2], Ermia E. Melika[4], Andrew K. Tawadros[4], Aliza Mujahid[4], Jacob Sandler[1,2], Kenneth M. Pryse[1,2], Justin M. Sacks[7], Elliot L. Elson[1,2,6], Guy M. Genin[1,2,3,#], Farid Alisafaei[1,4,#]

1. NSF Science and Technology Center for Engineering Mechanobiology
2. Department of Mechanical Engineering and Materials Science, Washington University in St. Louis
3. Department of Biomedical Engineering, Washington University in St. Louis
4. Department of Mechanical Engineering, New Jersey Institute of Technology
5. Department of Pathology, Saint Louis University School of Medicine
6. Department of Biochemistry and Molecular Biophysics, Washington University in St. Louis School of Medicine
7. Division of Plastic and Reconstructive Surgery, Washington University in St. Louis School of Medicine

Corresponding authors: farid.alisafaei@njit.edu, genin@wustl.edu
* These authors contributed equally to this work.

Abstract. Surgical repair of chronic wounds often requires split-thickness skin grafts in which epidermis and a thin part of the dermis from one site are harvested, cut into a meshwork, and stretched to cover a larger wound area. The main drawback of split-thickness skin grafting is excessive contracture of the skin graft in the wound site which is caused by the long-term activation and transition of low-contractile fibroblasts to hyper-contractile myofibroblast cells. To test whether there is a relationship between graft preparation and long-term graft contracture, we hypothesized that the strain field that cells experience within a meshed graft regulates the activation of fibroblasts, and that the strain field and therefore cell activation level can be tailored by adjusting the meshing configurations to control the graft contracture. To test the hypothesis, we estimated strain fields of skin grafts with a wide range of clinically relevant meshing configurations, and evaluated the responses of human dermal fibroblasts to these strain levels within skin tissue constructs. We found a previously unknown role of the extracellular collagen matrix in the development of mechanical memory in fibroblasts and their long-term activation level. Using an integrated experimental and theoretical approach, we showed that time- and strain-dependent behavior of the extracellular collagen matrix determines the stress level that cells experience during skin tissue stretching and subsequently the cell activation level after tissue unloading.

Introduction

Many cells seemingly remember previous mechanical conditions through changes to gene or protein expression that persist over physiologically relevant timescales [1–7]. Much work in the field of mechanobiology points to mesenchymal stem cells remembering the stiffness of their two-dimensional (2D) substrates to which they adhere through integrin ligation, affecting aspects of subsequent differentiation [2–4]. Culturing stem cells on 2D substrates showed that both stiff and soft substrates can induce mechanical memory in stem cells, enabling them to retain the signature of their past substrate stiffness even after moving to a new substrate with different stiffness [5,6]. In addition to stem cells, fibroblasts can also develop mechanical memory and remember the stiffness of their past 2D substrate, even for a longer time compared with stem cells. For example, lung fibroblasts, exhibiting high contractility and activation levels on stiff substrates, retained their pro-fibrotic myofibroblast signature for weeks even after exposure to soft substrates [1].

In addition to the stiffness of their extracellular matrix, fibroblasts also experience other mechanical signals in the body such as external forces [8], and we hypothesized that this would have effects in the form of long-term activation or deactivation of fibroblasts. These forces on fibroblasts are often in the form of long-term static loading [8,9]. While only cyclic dynamic loading (and not static loading) induced mechanical memory in stem cells [10], it remains unknown whether fibroblasts can develop and maintain mechanical memory under static loading. Furthermore, these external and long-term static forces are transmitted to fibroblasts through their three-dimensional (3D) extracellular environment whose physical properties are known to change with the magnitude and duration of the external loading [11–13]. Therefore, we studied whether fibroblasts can develop and maintain mechanical memory under static loading within physiologically-relevant 3D extracellular matrice.

An area where this is particularly important is skin grafting surgeries. Each year only in America 8.2 million suffer a chronic wound arising from burns, diabetic ulcers, skin cancer surgery, or infection [14,15]. These fail to pass through the normal healing process and the body is not able to replace the damaged skin at the wound site [16–20]. To protect the wound from the environment and pathogens, larger chronic wounds are often treated with split-thickness skin grafts which consist of the epidermis and a thin part of the dermis taken from a donor or from one part of the body (Fig. 1A (i)), and then meshed with rows of small interrupted slits (Fig. 1A (ii)), stretched (Fig. 1A (iii)), and transplanted over a larger wound site (Fig. 1A (iv)) [21–24]. In the process of skin grafting and as a result of skin graft stretching, fibroblast cells and their extracellular matrix experience static tensile strains. We hypothesized that this stretching of a meshed skin graft would lead to long-term activation or deactivation of cells depending on the magnitude and duration of tensile strain in the skin graft.

Results

The spatially varying strain fields experienced by cells in a skin graft can be controlled by changing the "meshing ratio". To test the hypothesis that the strain field within a graft varies with the meshing ratio, we evaluated how the strain field in a skin graft is affected by altering grafting parameters such as meshing ratio (Fig. 1B). Note that skin is not an isotropic material as it has orientation-dependent mechanical properties (Fig. 1C). This includes a critical effect of Langer's lines, also called cleavage lines, in different parts of the body. Langer's lines are topological lines that parallel the dominant orientation of collagen fibers and fibroblast cells in the dermis [25–30]. Skin grafts are harvested from the donor site in an orientation relative to the Langer's

lines depending on the availability of the donor site and the wound size. For example, Fig. 1C shows skin grafts harvested from the donor site in two different orientations: perpendicular and parallel to the Langer's lines. As expected, mechanical testing of two such skin grafts shows that skin stretching in the direction of Langer's lines requires higher forces,[31] as collagen fibers are aligned in the direction of Langer's line and therefore the tissue exhibits higher stiffness in this direction (Fig. 1C) [32].

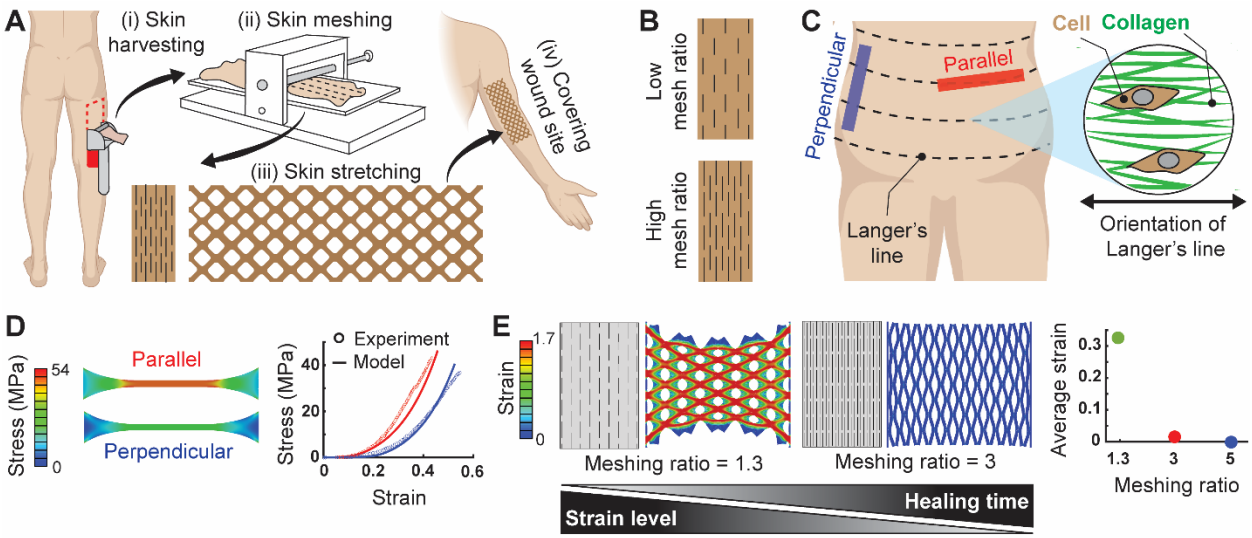

Figure 1. The strain level that skin tissues experience during skin graft stretching can be tailored by an order of magnitude by tuning skin graft meshing ratio. (A) Skin grafting is an example of medical procedures where skin tissues experience long-term external stretching. To protect from pathogens, large chronic wounds are often treated with split-thickness skin grafts in which epidermis and part of the dermis are harvested from a donor site (i), then cut into a meshwork of slits (ii) and stretched (iii) over a larger wound site (iv). (B) A skin graft can be meshed with different meshing ratios to cover a wound with a specific area. However, the choice of meshing ratio will impact the strain field that cells experience in the stretched skin graft. (C) Skin is an anisotropic material with orientation-dependent mechanical properties where fibroblast cells and collagen fibers are mainly aligned along topological lines called Langer's lines. (D) To determine how the strain field in skin grafts changes with meshing ratio, we first calibrated a hyperelastic model against uniaxial stretching experiments of unmeshed skin grafts. (E) We then used the calibrated model to determine how the strain field changes with meshing ratio. The simulations showed the strain fields generated in skin tissues depend strongly on the design of slits with the choice of meshing ratio affecting the average strains in graft tissue by an order of magnitude. (Strains and stresses in D and E represent the maximum principal strain and stress, respectively.)

This anisotropic behavior of the skin can be approximated by hyperelastic anisotropic continuum models [33,34] calibrated by fitting to unmeshed skin stretching experiments, and implemented into a finite element framework (Fig. 1D). Using the calibrated skin model, we found that the strain distribution in meshed skin grafts depends strongly on the meshing ratio (Fig. 1E). Skin meshed with higher meshing ratios has higher numbers and longer cuts, and can be stretched easily without undergoing high tensile strains. Note that meshing ratios of 1 to 5 are frequently used in skin graft surgeries [35] and our results show that the choice of meshing ratio can induce more than an order of magnitude change in the average strain level in skin tissues with average strains of over 30% possible (Fig. 1E).

Stretching skin tissues can induce long-term changes in the tendency of the tissue to contract, depending on the magnitude and duration of tissue stretching. We next studied whether the 30% change in the strain level of skin tissues can affect their tendency to contract on a long timescale. To this end, we created thin anisotropic skin tissues made of dermal fibroblast cells and type I collagen in a Teflon mold (Fig. 2A). The tissues were compacted over 2 days and formed thin contractile rings with cells aligned in the circumferential direction (Fig. 2C-2D), similar to the alignment of cells along the Langer's line in the body (Fig. 1C).

To measure how the long-term tissue contractile force changes with the externally-applied strain level in skin tissues, we first measured the tissue contractile force F^0 on day 2 (Fig. 2B (i)). We then statically exposed the tissues to low (0 %), medium (5 %), and high (30 %) strain levels for either 24 hours (long stretching duration) or 1 hour (short stretching duration) (Fig. 2B (ii)), followed by releasing the load for one day (Fig. 2B (iii)). Finally, we measured the tissue contractile force F^0 again (Fig. 2B (iv)) to determine whether being exposed to tensile strains has induced a permanent change in the contractility levels of the skin tissues.

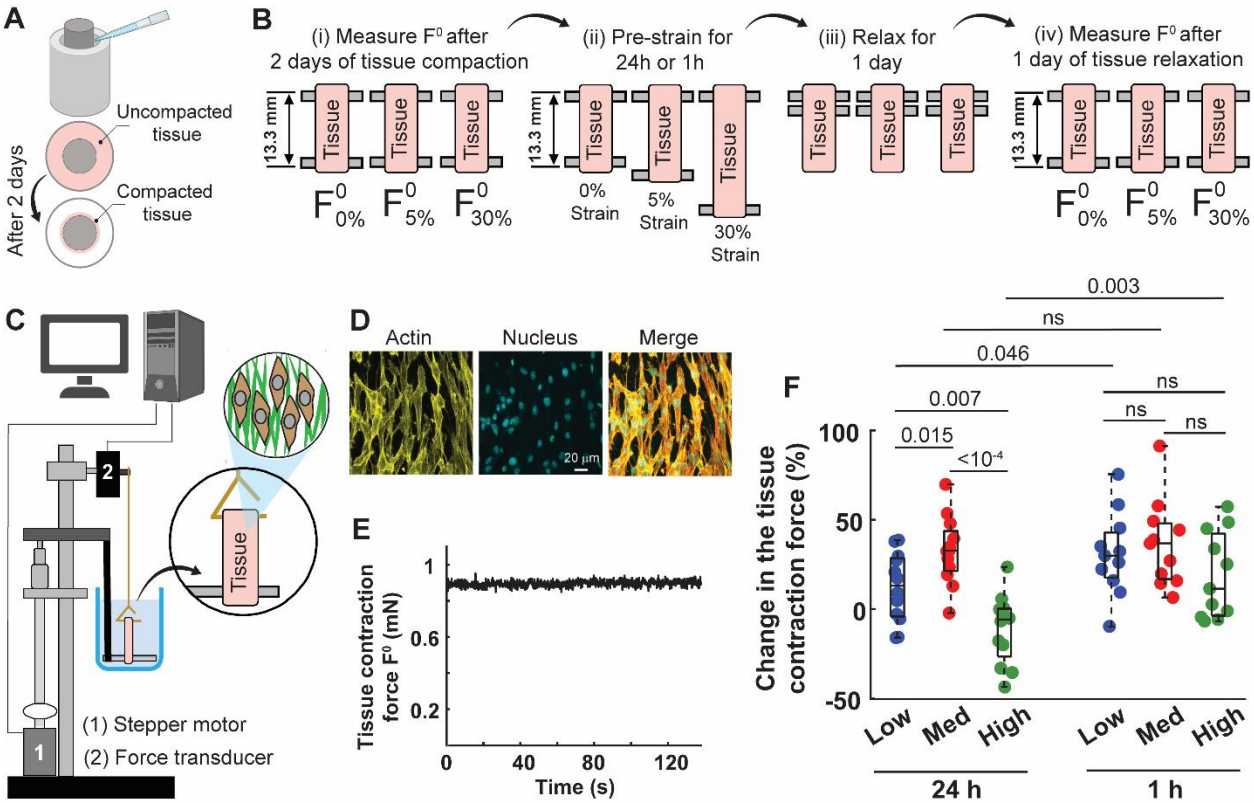

Figure 2. Stretching skin tissues for a long duration can induce long-term changes in the tissue contractile force in a biphasic manner with tissue strain level. (A) To study whether the externally-generated strain field in a skin tissue affects the long-term behavior of the tissue, we created thin anisotropic tissues made of dermal fibroblast cells and type I collagen in a Teflon mold. The tissues were compacted over 2 days and formed thin contractile rings with cells aligned in the circumferential direction. (B) To measure how the externally-applied strain field affects the long-term tendency of tissues to contract, we first measured the tissue contractile force F^0 on day 2 (i). We then statically exposed the tissues to low (0 %), medium (5 %), and high (30 %) strain levels for either 24h (long stretching duration) or 1h (short stretching duration) (ii), followed by releasing the load for 1 day (iii), and measurement of F^0. All measurements of the tissue contractile force F^0 were performed at a tissue length of 13.3 mm. At this length, the periphery of the tissues on the stretcher device is equal to the periphery of the tissues in the mold on day 2. (C) The measurements of the tissue contractile force were performed using a custom-made device with a temperature-controlled organ bath. (D) Skin tissues exhibit anisotropic mechanical properties due to

the pre-alignment of cells. (E) A representative plot of tissue force measurements. The tissue contractility level was determined as the tissue contractile force F^0 measured upon hanging the tissue ring on the device. (F) The change in the tissue contractile force [F^0(iv) - F^0(i)] / F^0(i) was measured to determine the effect of pre-strain level on long-term tissue contractility. Tissues pre-strained for the long duration (and not for the short duration) exhibited a biphasic trend in long-term tissue contractility with pre-strain magnitude. (*n* is 12 and 11 for the groups under the long duration (24h) and short duration (1h) of pre-straining, respectively.)

We found that tissues pre-strained for the short duration did not show any strain-dependent changes in their long-term tendency to contract and they all showed a similar level of tissue contractile force after one day of unloading independent of the tissue pre-strain magnitudes (Fig. 2F). However, the contractile force of the tissues pre-strained for the long duration showed a surprising biphasic trend with pre-strain magnitude (Fig. 2F), indicating that tissue pre-strain magnitude may induce mechanical memory in cells and change their activation levels in a non-monotonic manner.

Time- and strain-dependent physical properties of the extracellular matrix regulate long-term cell activation and tissue contractility. We hypothesized that the time- and strain-dependent changes in tissue contractility in Fig. 2F are regulated by the extracellular collagen matrix as its physical properties are known to change with the magnitude and duration of strain. We thus measured the physical properties of our tissues (Fig. 3A (v)) and their collagen matrices (Fig. 3A (vii)) to test how they changed with the magnitude and duration of tissue pre-straining (Figs. 3A-3B). To this end, we used a stress relaxation test where the sample is kept under a fixed small strain while the build-up and subsequent relaxation of stress in the sample are recorded over time (Fig. 3B). Furthermore, this test allows us to measure the steady-state stiffness of the sample as described in Fig. 3B.

We found that the tissues pre-strained for the short duration had similar physical properties independent of the tissue pre-strain magnitudes (Figs. 3D-3E), indicating that stretching of tissues even up to 30% strain for a short time does not cause permanent changes in the tissue's physical properties. However, the tissues pre-strained for 24h (long duration) showed a slight change in the tissue's physical properties when the magnitude of tissue pre-strain was high (Fig. 3C). To test whether this change in the tissue's physical properties is due to alterations in the stiffness of the extracellular collagen matrix, we treated the tissues with actomyosin inhibitors to disrupt the actomyosin contractility of the cells, thereby decoupling the effects of cell force and matrix [36]. Our results showed that all tissues pre-strained for 24h (long duration) had significantly softer matrix compared with the ones pre-strained for 1h (Figs. 3F-3H). Also, unlike the 1h pre-strained tissues, the tissues pre-strained for 24h exhibited matrix softening with tissue pre-strain magnitude. This was shown in Figs. 3F-3H where the 24h pre-strained tissue with high strain magnitude had a remarkedly softer matrix compared with the ones pre-strained for 24h but with low or medium magnitude. These results demonstrated that stretching of tissues for a short time does not cause permanent changes in the matrix's physical properties and the matrix shows a full elastic recovery after the tissue is unloaded. However, stretching of tissues for a long time causes softening of the matrix, and the softening increases with tissue stretching magnitude.

Time- and strain-dependent physical properties of the extracellular matrix regulate the stress level that cells experience in stretched skin tissue. To understand the underlying mechanism of the time- and strain-dependent tissue contractility in Fig. 2F, we developed a predictive theoretical framework that includes an active bio-chemo-mechanical tissue model (Fig. 4) coupled with a signaling network model (Fig. 6A). When tissue is stretched, external forces are transmitted to the cells through the extracellular matrix whose properties are known to change with magnitude and duration of stretching. Therefore, we used the theoretical framework to

answer (i) how the transmission of external forces to the cells changes with magnitude and duration of tissue stretching, and (ii) how these changes in force transmission impact cellular memory and long-term activation of cells.

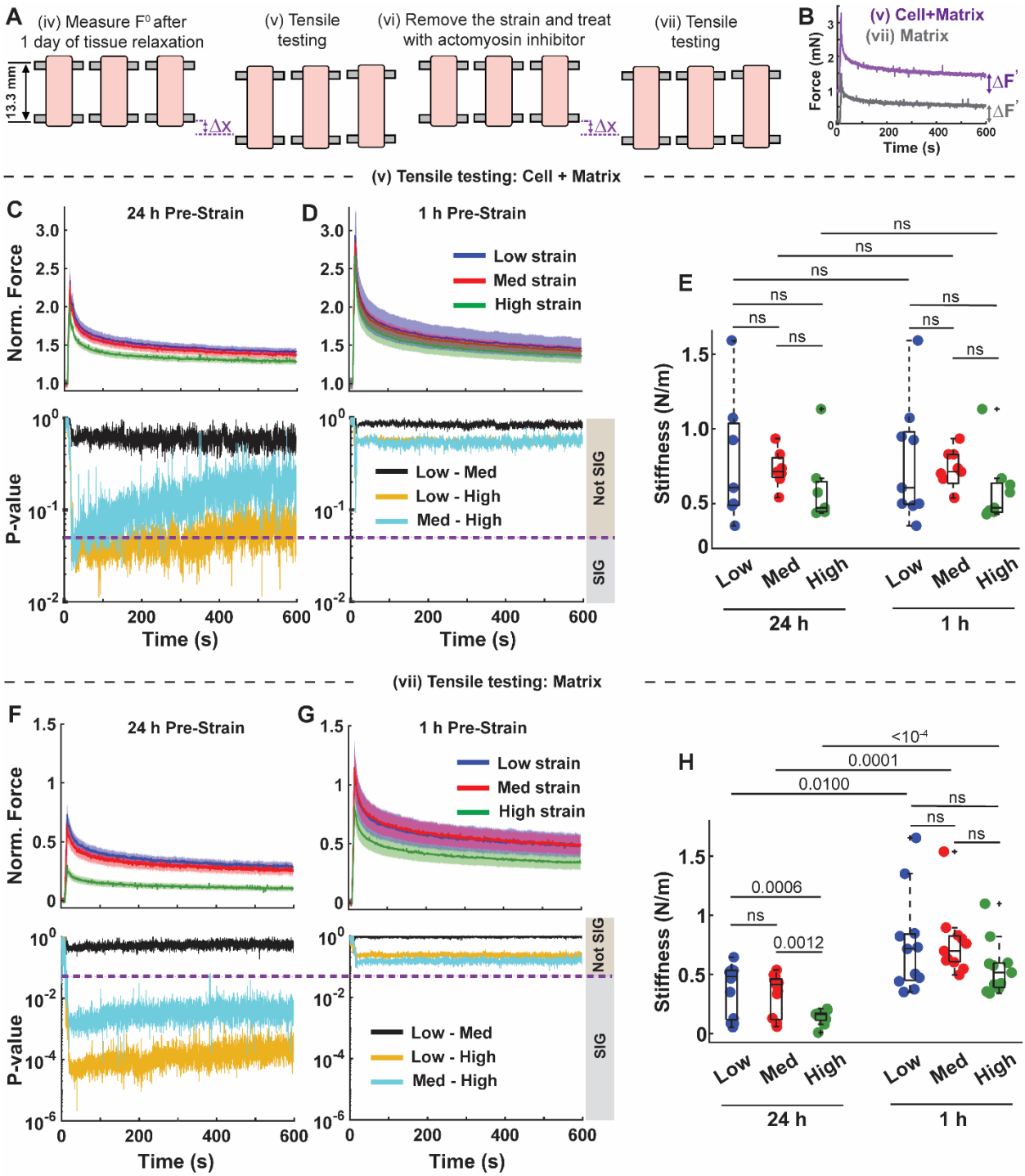

Figure 3. Physical properties of the extracellular collagen matrix change with magnitude and duration of tissue stretching. (A) The physical properties of the pre-strained tissues were determined with (v) and without (vii) the presence of cellular contractile forces using a stress relaxation test. (B) Representative plots of tissue responses to the stress relaxation test before (purple line) and after (gray

line) disruption of cell contractile forces. Tissue stiffness is determined as $\Delta F'/\Delta X$. (C-E) The physical properties of the tissues pre-strained for 1h showed no significant changes with pre-strain magnitude, while slight softening was observed with increasing pre-strain magnitude in the tissues pre-strained for 24h. (F-H) Disruption of cell contractile forces revealed significant softening of the extracellular matrix in the tissues pre-strained for 24h with the matrix softening further increasing with tissue pre-strain magnitude. (In C-E, *n* is 7 and 9 for the 24h and 1h groups, respectively. In F-H, *n* is 13 and 11 for the 24h and 1h groups, respectively. In C, D, F, and G, the solid lines and the shaded areas represent the mean and standard error, respectively.)

The active bio-chemo-mechanical tissue model is composed of extracellular matrices and an active force-generating cell model (Fig. 4A) which were developed based on the following three experimentally-supported hypotheses. First, the matrix exhibits long-term time-dependent behavior under tension. To test this hypothesis, we performed the matrix stress relaxation test in Fig. 3G over a much longer timescale and we found that stress in the matrix continues to decrease with time, resulting in more than a 30% drop in matrix stress over 1h (Fig. 4B). The time-dependent behavior of the matrix in tension was accounted for in the model by adding a viscous element to the matrix element in tension (Fig. 4A). Second, the matrix stiffness changes with magnitude of tensile matrix strain. To test this hypothesis, we stretched the matrix at a slow rate to determine its time-independent stiffness. Our experiments showed an initial strain-stiffening followed by a softening region at large strains demonstrated by decreases in the slope of the force-strain curve (Fig. 4C). The strain-dependent behavior of the matrix in tension was accounted for in the model by adopting the stress-strain relationship in Fig. 4C as the constitutive model of the matrix element in tension. Third, cell actomyosin contractility and thus cell-generated contractile force increase with the level of tension caused by either external tensile forces or external resistance from the matrix against cell contraction (Fig. 4D). This is mathematically represented in our model where cell-generated contractile stress σ_c increases with the tissue stress σ. This hypothesis is supported by our previous live-cell imaging experiments [37] and others [38] where stretching of cells was found to be correlated with an increase in actin intensity in the direction of stretching. The hypothesis is also supported by our previous 2D studies [39] and others [40,41] where increasing external resistance against cell contraction arising from higher matrix stiffness caused higher tension at the cell-matrix interface, which in turn promoted cell actomyosin contractility and cell force generation.

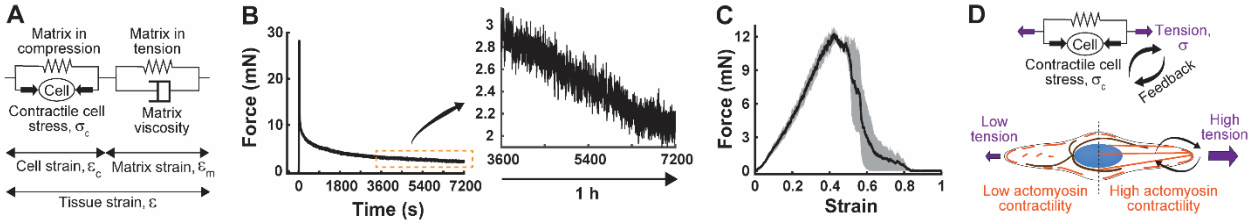

Figure 4. Determination of time- and strain-dependent physical properties of the extracellular collagen matrix. (A) A one-dimensional representation of the active bio-chemo-mechanical tissue model. The model is composed of an active force-generating element (cell) connected to two passive elements which represent the matrix parts that are under compression and tension due to cell contraction in the absence of external strain ($\varepsilon = 0$). The model elements were developed based on the following three experimentally-supported hypotheses. (B) First, the extracellular collagen matrix exhibits long-term time-dependent behavior under tension. (C) Second, the stiffness of the extracellular collagen matrix changes with matrix strain magnitude as demonstrated by an initial increase in the slope of the curve at small strains followed by a softening region and decreases in the slope at large strains (*n* = 3, the solid line and the

shaded area represent the mean and standard error, respectively). (D) Third, cell actomyosin contractility and thus cell contractile force increase with tension.

In a tissue stretched with a fixed strain ε, the matrix element in tension (Fig. 4A) is stretched by both cell-generated contractile stress σ_c and the external strain ε. However, due to the viscous nature of the collagen matrix characterized in Fig. 4B, the tensile strain in the matrix, ε_m, increases with stretching duration (Fig. 5A). As a result, for long stretching durations (e.g., 24h), the matrix can be overstretched which in turn damages the matrix microstructures and causes matrix softening. This was shown in our simulations where, after 1h tissue stretching, the matrix was undamaged and thus the slopes of the stress-strain curve (m) were high and independent of the tissue strain magnitude ε, while m significantly dropped after 24h stretching with m further decreasing with ε (Fig. 5B). To directly compare the model predictions with our experiments in Fig. 3H, we calculated the matrix stiffness (*k*) in N/m unit, and we found the model predictions to be in excellent agreement with our experiments (Fig. 8B), explaining the physical mechanism through which matrix stiffness changes with magnitude and duration of tissue stretching.

The model also showed how the changes in the matrix stiffness affect the tension generated in the tissues, σ, and subsequently cell stress σ_c (Fig. 5C). During the first hours of tissue stretching (e.g., time = 1h), the matrix remains undamaged independent of the tissue strain magnitude ε and thus the stress generated in the tissue σ monotonically increases with the tissue strain magnitude ε (Fig. 5C). However, increasing the duration of tissue stretching (e.g., time = 24h) results in over-stretching of the matrix which in turn damages and softens the matrix. The softening of the matrix increases with the tissue strain magnitude ε such that for high ε, the stress generated in the tissue, σ, significantly drops, which in turn decreases cell actomyosin contractility and cell-generated stress σ_c (Fig. 5C). Taken together, our results showed how the time- and strain-dependent changes in the matrix stiffness alter the stress generated in a stretched tissue, which in turn affects the stress level that cells experience.

The magnitude and duration of the stress that cells experience in a stretched skin tissue determine their long-term activation level. We next studied how the magnitude and duration of the stress that cells experienced in our stretched skin tissues can affect the long-term activation level of the cells after unloading the tissues. To this end, we developed a signaling network model (Fig. 6A) and coupled it with the active tissue model such that the signaling model takes the duration and magnitude of stress that cells experience in stretched tissues from the active tissue model as input (Fig. 6B). The signaling network model was directly developed based on a cascade of known biological processes described briefly here.

First, tensile stress on cells is known to promote cell actomyosin contractility through pathways such as Rho-Rock or activation of mechanosensitive ion channels (Fig. 6A i) [42–45]. While excessive cell contraction can cause detachment of the cell from the extracellular matrix [46] and thus switching to a transcriptionally less active state (Fig. 6A v and viii) [8], modest increases in cell actomyosin contractility lead to translocations of transcriptional and epigenetic factors (e.g., MKL and YAP/TAZ) to the nucleus (Fig. 6A iv) which in turn promotes transcription of genes associated with actomyosin contractility and cell activation (Fig. 6A vi and vii) [47]. Finally, the expression of the activation genes increases cell actomyosin contractility which is captured in our model through a feedback loop (Fig. 6A ii and iii).

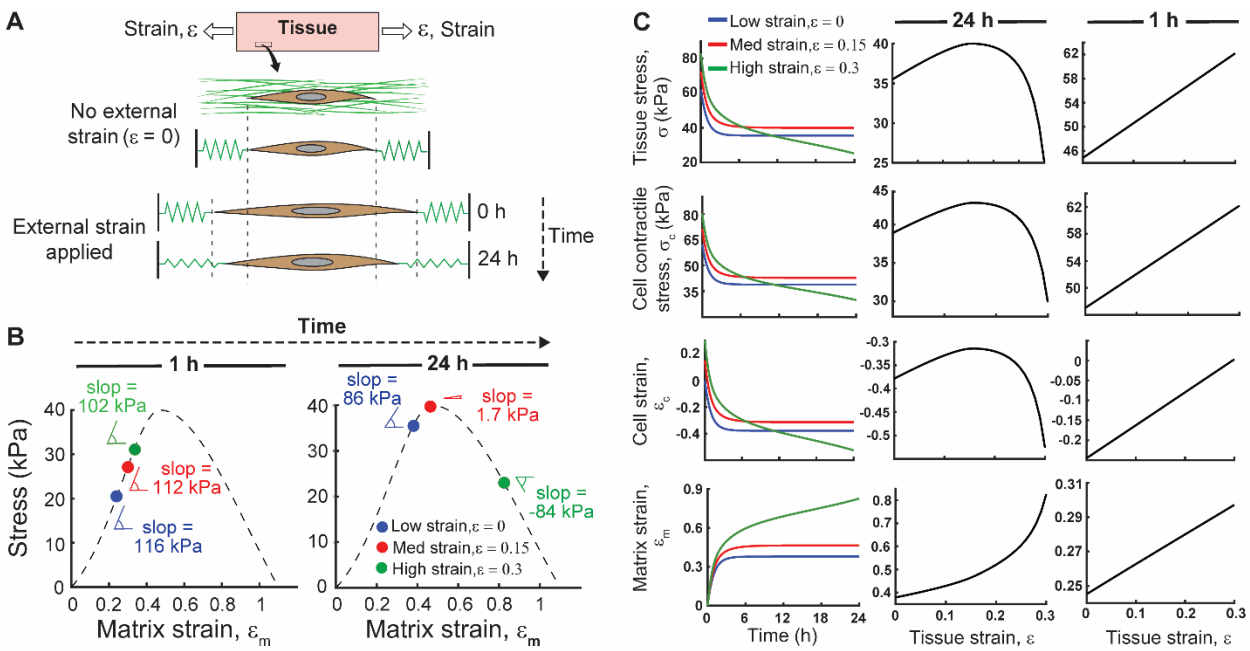

Figure 5. The stress level that cells experience in stretched skin tissues is regulated by the time and strain-dependent properties of the extracellular matrix. (A) In a stretched skin tissue, the viscous nature of the extracellular collagen matrix causes an increasing tensile strain in the matrix with tissue stretching duration. (B) This increase in the matrix strain ε_m over time can cause overstretching of the matrix for long stretching durations (e.g., time =24h), resulting in damage and softening of collagen matrices as represented by the decrease in the slopes of the stress-strain curve. The dashed line represents the constitutive behavior of the collagen matrix based on our experimental tests. (C) The matrix softening increases with the tissue strain magnitude ε such that for high ε, the stress generated in the tissue, σ, and thus the cell stress, σ_c, significantly drop, resulting in a biphasic trend with ε. On the contrary, during the first hours of tissue stretching (e.g., time = 1h), the matrix remains undamaged independent of the tissue strain magnitude ε and thus the stress generated in the tissue σ and the stress that cells experience σ_c monotonically increases with the tissue strain magnitude ε.

The input to the signaling network model is the stress that cells experienced "during" tissue stretching (Fig. 6A). This was determined by the active tissue model in Fig. 5C and was plotted for 1h and 24h tissue stretching durations in Fig. 6B. The output of the signaling network model is the level of actomyosin contractility in cells "after" releasing the tissues. Cells that underwent tension for 24h, developed mechanical memory and exhibited high activation levels after releasing the tissue if the tension magnitude during tissue stretching was not too low (Fig. 6B). On the contrary, cells that experienced tension for 1h, exhibited low activation levels after tissue unloading, although the tension magnitude during tissue stretching was very high. The model predictions are summarized in Fig. 6C which demonstrates how the duration and magnitude of tension that cells experience in a stretched tissue determine the level of cell activation one day after releasing the tissue.

Stretching skin tissues for a long duration can cause long-term activation of cells in a non-monotonic manner with tissue strain magnitude. The theoretical framework predicted that, for short durations of tissue stretching (e.g., 1h), cells experienced high tension during the tissue stretching (Fig. 6B, top), but due to the short duration of stretching, they did not develop mechanical memory and thus exhibited low activation levels after tissue unloading (Figs. 6B-6C). For long durations of tissue stretching (e.g., 24h), the tension that cells experienced during the

tissue stretching significantly dropped for high tissue strain magnitude (Fig. 6B, top), and therefore only cells under low and medium tissue strain magnitudes exhibited high activation levels after tissue unloading (Figs. 6B-6C). To validate the model predictions (Fig. 8A which is a replot of Fig. 6B (bottom) on day 2 after tissue unloading), we fixed our tissues one day after tissue unloading and stained them with F-actin (Fig. 7A) and α-SMA (Fig. 7B) which are well-known indicators of fibroblast activation level. Our results were all consistent with the model predictions demonstrating that the long-term activation of cells is determined by the duration and magnitude of the stress that cells experience in tissues.

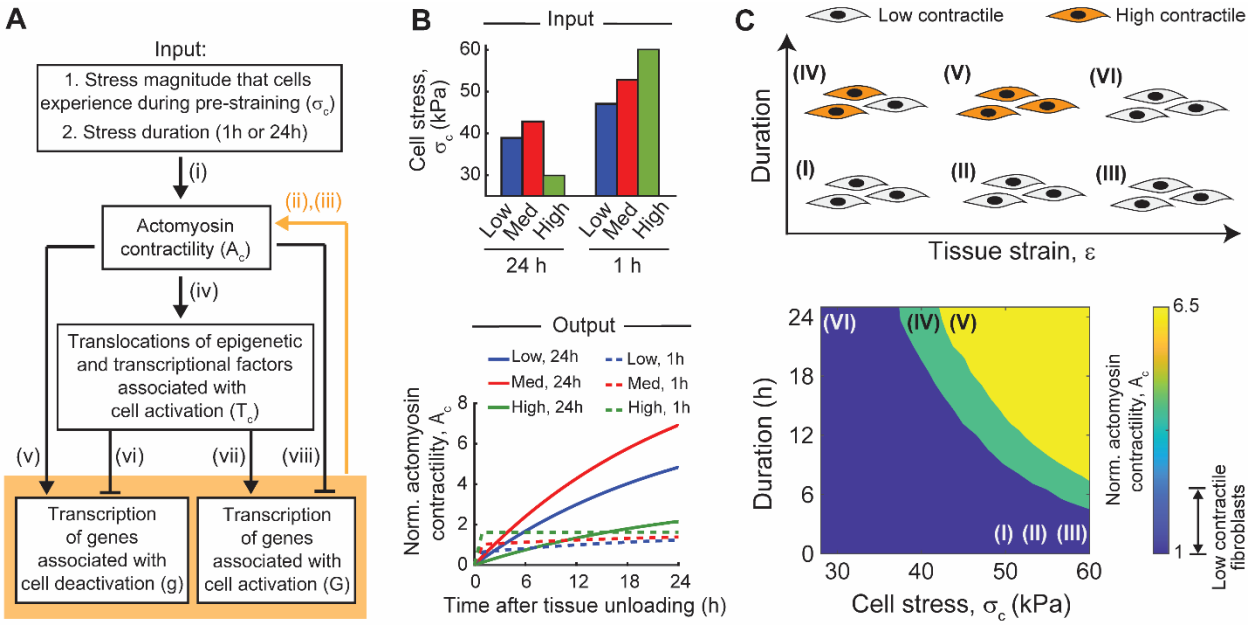

Figure 6. The magnitude and duration of the stress that cells experience in stretched skin tissues determine cellular mechanical memory induction and long-term activation of fibroblasts. (A) A signaling network model to predict the level of cell activation after releasing the tissues. (B) The input to the model is the duration (1h or 24h) and magnitude of stress that cells experience in stretched tissues determined by the active tissue model in Fig. 5C. The model predicts that cells that undergo tension for 24h (long duration) develop mechanical memory and show high activation levels after releasing the tissue if the magnitude of the tension during tissue stretching is not too low. On the contrary, cells that experience tension for 1h (short duration) exhibit low activation levels after tissue unloading although the tension magnitude during tissue stretching is very high. (C) The dependence of cellular memory and cell activation level on the magnitude and duration of tension is depicted in a phase diagram predicted by the signaling network model. Each of the six tissues is shown in the phase diagram.

Long-term tissue contraction force depends on both cell activation level and matrix stiffness after tissue unloading. Our experiments (Fig. 7A) and theory (Fig. 8A) showed that stretching the tissue for 24h (long duration) with low or medium tissue strain magnitude induced mechanical memory in cells, resulting in long-term activation of cells in Low/24h and Med/24h tissues. This was shown by the higher actomyosin contractility levels of cells in these tissue 1 day after tissue unloading. However, measuring the tissue contractile forces 1 day after unloading the tissues showed that the long-term tendency of Low/24h and Med/24h tissues are slightly less and similar to the one in 1h groups, respectively (Fig. 2F). Out theoretical framework showed that this is caused by the softening of the matrix in Low/24h and Med/24h tissues as the tissue contractility depends on both cell activation level and matrix stiffness. While the cell activation level

determines the level of cell contractility and force generation, the matrix stiffness regulates the transmission of these contractile forces. This is shown in Fig. 8 where we used our theoretical framework to determine the tissue contractile stress (σ) 1 day after tissue unloading (and not during the tissue stretching as in Fig. 5C). The model predictions showed good agreement with our experiments in Fig. 2F and revealed that high levels of cell activation and cell contractility do not necessarily lead to a high tissue contraction level, and the stiffness of the matrix plays a key role in the transmission of cellular forces through the tissue and subsequently the tendency of the tissue to contract. Therefore, as the tissues under long stretching duration exhibit matrix softening, the contractile forces generated by individual cells cannot be effectively transmitted through the tissue to generate a large tissue contraction force.

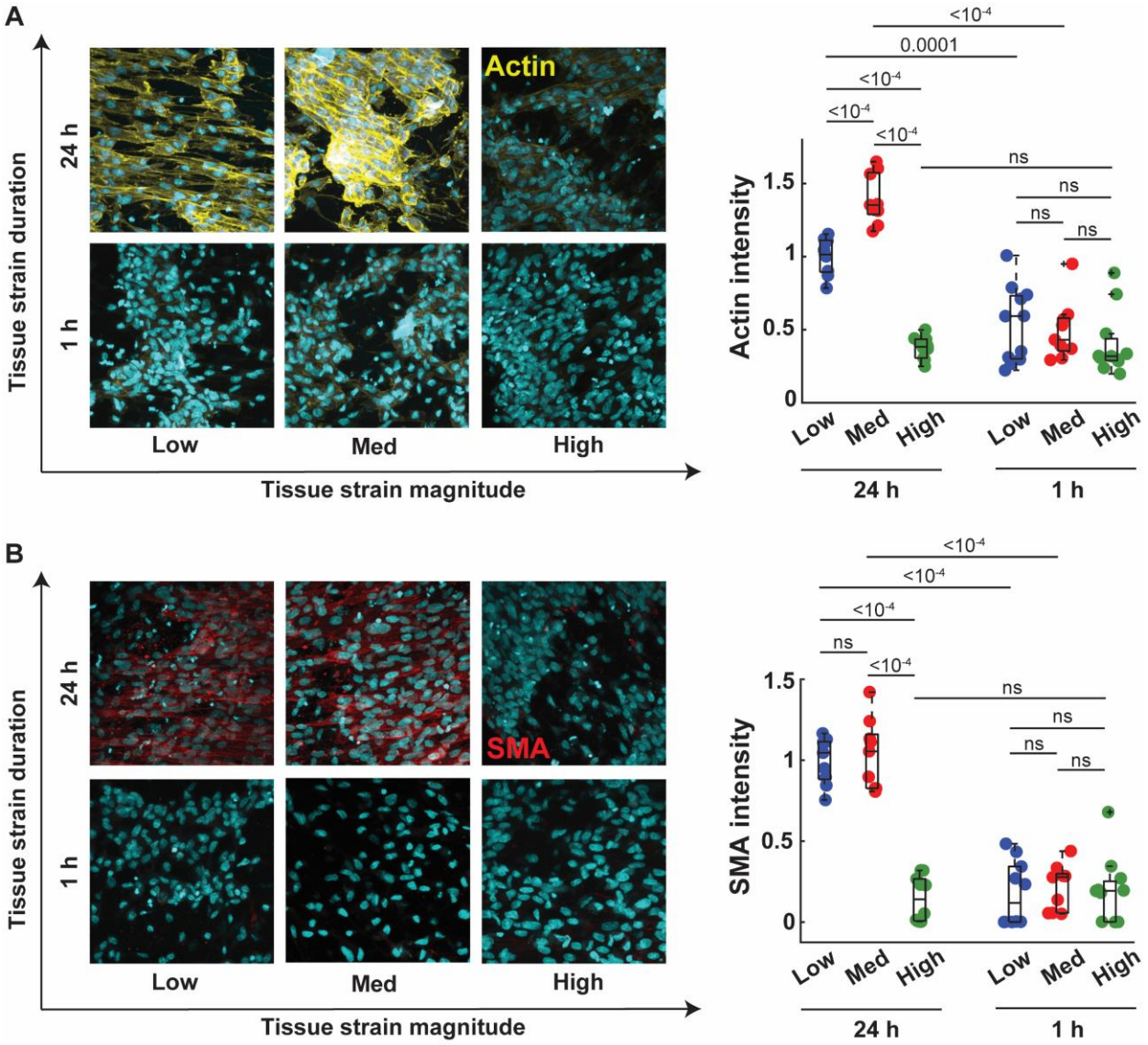

Figure 7. Stretching skin tissues for a long duration can induce mechanical memory in cells and cause their long-term activation in a non-monotonic manner with tissue strain magnitude. To determine the level of cell activation, the expression levels of F-Actin and α-SMA in fibroblasts were measured. Tissues were fixed 1 day after tissue unloading and were stained with F-actin and α-SMA which are well-known indicators of fibroblast activation level.

Conclusions

Using an integrated experimental and theoretical approach, we provided a physical mechanism for the long-term activation of cells and tissue contractility, which are known to play key roles in wound healing and diseases such as fibrosis. Unlike previous studies on stem cells, we showed that fibroblasts can develop mechanical memory under static tissue strain, depending on the duration and magnitude of tissue strain. We reported a previously unknown role of the extracellular matrix in the development of mechanical memory in fibroblasts and their long-term activation. We found that the time- and strain-dependent physical properties of the matrix determine the stress level that cells experience during tissue stretching and subsequently the cell activation level after tissue unloading.

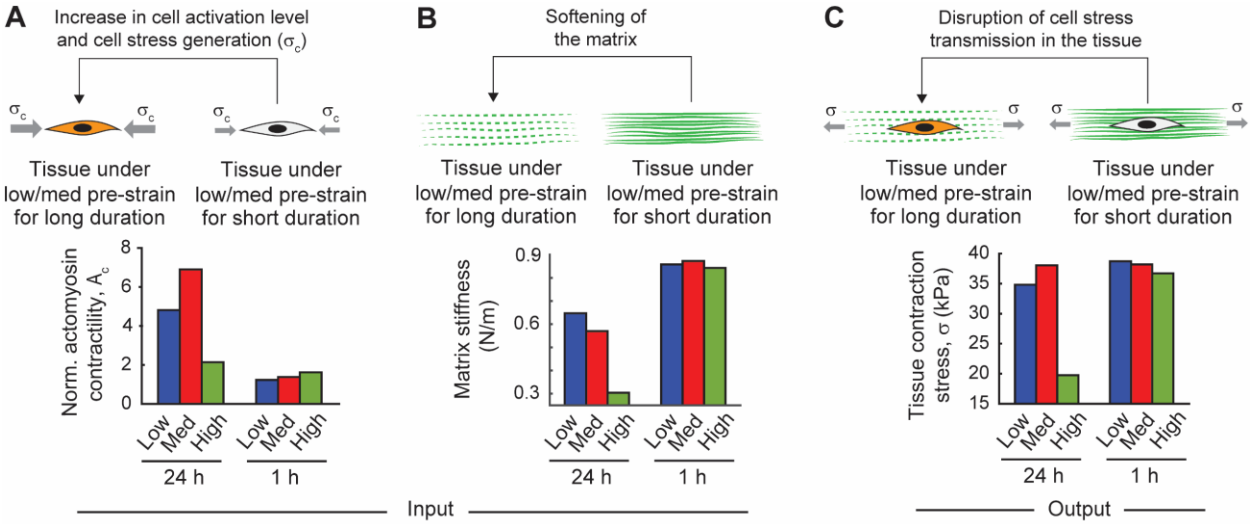

Figure 8. Tissue contraction force depends on both cell activation level and matrix stiffness. (A) First, cell activation levels 1 day after tissue unloading are plotted for each of the tissues. The model predictions for cell activation levels are in excellent agreement with the experimental measurements of cell contractility biomarkers in Fig. 7. (B) Second, matrix stiffness predicted by the model in Fig. 5B is plotted in N/m unit for each of the tissues. The model predictions agree well with the experimental measurements of matrix stiffness in Fig. 3H. (C) Finally, the cell activation levels and matrix stiffness are used to predict the tissue contraction force 1 day after tissue unloading. The model shows that a high level of cell activation and cell contractility does not necessarily lead to a high tissue contraction level, and the stiffness of the matrix plays a key role in the transmission of cellular forces through the tissue and thus the tendency of the tissue to contract. Therefore, as the tissues under long stretching duration (24h) exhibit matrix softening, the contractile forces generated by individual cells cannot be effectively transmitted through the tissue to generate a large tissue contraction force. As a result, the tissue with the highest cell activation level but softened matrix (Med/24h) exhibits a tissue contraction force similar to the ones generated by the tissues with low cell activation levels but with intact matrices (1h groups). The model predictions for the tissue contraction force are consistent with the experimental measurements in Fig. 2F.

References

1. Balestrini, J. L., Chaudhry, S., Sarrazy, V., Koehler, A. & Hinz, B. The mechanical memory of lung myofibroblasts. *Integrative Biology* **4**, 410–421 (2012).

2. Zhang, C. *et al.* Mechanics-driven nuclear localization of YAP can be reversed by N-cadherin ligation in mesenchymal stem cells. *Nat Commun* **12**, 6229 (2021).
3. Killaars, A. R. *et al.* Extended Exposure to Stiff Microenvironments Leads to Persistent Chromatin Remodeling in Human Mesenchymal Stem Cells. *Advanced Science* **6**, 1801483 (2019).
4. Heo, S.-J., Cosgrove, B. D., Dai, E. N. & Mauck, R. L. Mechano-adaptation of the stem cell nucleus. *Nucleus* **9**, 9–19 (2018).
5. Li, C. X. *et al.* MicroRNA-21 preserves the fibrotic mechanical memory of mesenchymal stem cells. *Nature Mater* **16**, 379–389 (2017).
6. Yang, C., Tibbitt, M. W., Basta, L. & Anseth, K. S. Mechanical memory and dosing influence stem cell fate. *Nature Mater* **13**, 645–652 (2014).
7. Almeida, J., Mathur, J., Lee, Y. L., Sarker, B. & Pathak, A. Mechanically primed cells transfer memory to fibrous matrices for invasion across environments of distinct stiffness and dimensionality. *MBoC* mbc.E22-10-0469 (2023) doi:10.1091/mbc.E22-10-0469.
8. Damodaran, K. *et al.* Compressive force induces reversible chromatin condensation and cell geometry–dependent transcriptional response. *MBoC* **29**, 3039–3051 (2018).
9. Wells, R. G. Tissue mechanics and fibrosis. *Biochimica et Biophysica Acta (BBA) - Molecular Basis of Disease* **1832**, 884–890 (2013).
10. Heo, S.-J. *et al.* Biophysical Regulation of Chromatin Architecture Instills a Mechanical Memory in Mesenchymal Stem Cells. *Sci Rep* **5**, 16895 (2015).
11. Chaudhuri, O., Cooper-White, J., Janmey, P. A., Mooney, D. J. & Shenoy, V. B. Effects of extracellular matrix viscoelasticity on cellular behaviour. *Nature* **584**, 535–546 (2020).
12. Hall, M. S. *et al.* Fibrous nonlinear elasticity enables positive mechanical feedback between cells and ECMs. *Proceedings of the National Academy of Sciences* **113**, 14043–14048 (2016).
13. Alisafaei, F., Chen, X., Leahy, T., Janmey, P. A. & Shenoy, V. B. Long-range mechanical signaling in biological systems. *Soft Matter* **17**, 241–253 (2021).
14. Sen, C. K. Human Wounds and Its Burden: An Updated Compendium of Estimates. *Advances in Wound Care* **8**, 39–48 (2019).
15. Sen, C. K. Human Wound and Its Burden: Updated 2020 Compendium of Estimates. *Advances in Wound Care* **10**, 281–292 (2021).
16. Frykberg, R. G. & Banks, J. Challenges in the Treatment of Chronic Wounds. *Advances in Wound Care* **4**, 560–582 (2015).
17. Siddiqui, A. R. & Bernstein, J. M. Chronic wound infection: Facts and controversies. *Clinics in Dermatology* **28**, 519–526 (2010).
18. Han, G. & Ceilley, R. Chronic Wound Healing: A Review of Current Management and Treatments. *Adv Ther* **34**, 599–610 (2017).
19. Powers, J. G., Higham, C., Broussard, K. & Phillips, T. J. Wound healing and treating wounds: Chronic wound care and management. *Journal of the American Academy of Dermatology* **74**, 607–625 (2016).
20. Li, M., Liang, Y., He, J., Zhang, H. & Guo, B. Two-Pronged Strategy of Biomechanically Active and Biochemically Multifunctional Hydrogel Wound Dressing To Accelerate Wound Closure and Wound Healing. *Chem. Mater.* **32**, 9937–9953 (2020).
21. Andreassi, A., Bilenchi, R., Biagioli, M. & D'Aniello, C. Classification and pathophysiology of skin grafts. *Clinics in Dermatology* **23**, 332–337 (2005).
22. Chuenkongkaew, T. Modification of Split-Thickness Skin Graft: Cosmetic Donor Site and Better Recipient Site. *Annals of Plastic Surgery* **50**, 212–214 (2003).
23. Lagus, H., Sarlomo-Rikala, M., Böhling, T. & Vuola, J. Prospective study on burns treated with Integra®, a cellulose sponge and split thickness skin graft: Comparative clinical and histological study—Randomized controlled trial. *Burns* **39**, 1577–1587 (2013).
24. Ayaz, M., Najafi, A. & Karami, M. Y. Thin Split Thickness Skin Grafting on Human Acellular Dermal Matrix Scaffold for the Treatment of Deep Burn Wounds. *Int J Organ Transplant Med* **12**, 44–51 (2021).
25. Ní Annaidh, A., Bruyère, K., Destrade, M., Gilchrist, M. D. & Otténio, M. Characterization of the anisotropic mechanical properties of excised human skin. *Journal of the Mechanical Behavior of Biomedical Materials* **5**, 139–148 (2012).
26. Gibson, T. Karl Langer (1819–1887) and his lines. *British Journal of Plastic Surgery* **31**, 1–2 (1978).
27. Carmichael, S. W. The tangled web of Langer's lines. *Clinical Anatomy* **27**, 162–168 (2014).

28. Langer, K. On the anatomy and physiology of the skin: I. The cleavability of the cutis. *British Journal of Plastic Surgery* **31**, 3–8 (1978).
29. Bush, M. A., Thorsrud, K., Miller, R. G., Dorion, R. B. J. & Bush, P. J. The Response of Skin to Applied Stress: Investigation of Bitemark Distortion in a Cadaver Model*. *Journal of Forensic Sciences* **55**, 71–76 (2010).
30. Bush, J., Ferguson, M. W. J., Mason, T. & McGrouther, G. The dynamic rotation of Langer's lines on facial expression. *Journal of Plastic, Reconstructive & Aesthetic Surgery* **60**, 393–399 (2007).
31. Ní Annaidh, A. *et al.* Automated Estimation of Collagen Fibre Dispersion in the Dermis and its Contribution to the Anisotropic Behaviour of Skin. *Ann Biomed Eng* **40**, 1666–1678 (2012).
32. Capek, L., Flynn, C., Molitor, M., Chong, S. & Henys, P. Graft orientation influences meshing ratio. *Burns* **44**, 1439–1445 (2018).
33. Gasser, T. C., Ogden, R. W. & Holzapfel, G. A. Hyperelastic modelling of arterial layers with distributed collagen fibre orientations. *Journal of The Royal Society Interface* **3**, 15–35 (2006).
34. Holzapfel, G. A., Gasser, T. C. & Ogden, R. W. A New Constitutive Framework for Arterial Wall Mechanics and a Comparative Study of Material Models. *Journal of Elasticity* **61**, 1–48 (2000).
35. Kan, T. *et al.* Calculation of practical skin donor area for meshed skin grafting in real-world surgery. *Dermatologic Therapy* **33**, e14393 (2020).
36. Wakatsuki, T., Kolodney, M. S., Zahalak, G. I. & Elson, E. L. Cell Mechanics Studied by a Reconstituted Model Tissue. *Biophysical Journal* **79**, 2353–2368 (2000).
37. Lee, S.-L. *et al.* Physically-Induced Cytoskeleton Remodeling of Cells in Three-Dimensional Culture. *PLoS ONE* **7**, e45512 (2012).
38. Icard-Arcizet, D., Cardoso, O., Richert, A. & Hénon, S. Cell stiffening in response to external stress is correlated to actin recruitment. *Biophys. J.* **94**, 2906–2913 (2008).
39. Alisafaei, F., Jokhun, D. S., Shivashankar, G. V. & Shenoy, V. B. Regulation of nuclear architecture, mechanics, and nucleocytoplasmic shuttling of epigenetic factors by cell geometric constraints. *PNAS* **116**, 13200–13209 (2019).
40. Ghibaudo, M. *et al.* Traction forces and rigidity sensing regulate cell functions. *Soft Matter* **4**, 1836 (2008).
41. Oakes, P. W., Banerjee, S., Marchetti, M. C. & Gardel, M. L. Geometry Regulates Traction Stresses in Adherent Cells. *Biophysical Journal* **107**, 825–833 (2014).
42. Lee, H. *et al.* The nuclear piston activates mechanosensitive ion channels to generate cell migration paths in confining microenvironments. *Science Advances* **7**, eabd4058 (2021).
43. Matthews, B. D. *et al.* Ultra-rapid activation of TRPV4 ion channels by mechanical forces applied to cell surface beta1 integrins. *Integr Biol (Camb)* **2**, 435–442 (2010).
44. Kobayashi, T. & Sokabe, M. Sensing substrate rigidity by mechanosensitive ion channels with stress fibers and focal adhesions. *Current Opinion in Cell Biology* **22**, 669–676 (2010).
45. Shenoy, V. B., Wang, H. & Wang, X. A chemo-mechanical free-energy-based approach to model durotaxis and extracellular stiffness-dependent contraction and polarization of cells. *Interface Focus* **6**, 20150067 (2016).
46. Alisafaei, F. *et al.* Tension anisotropy drives phenotypic transitions of cells via two-way cell-ECM feedback. 2022.03.13.484154 Preprint at https://doi.org/10.1101/2022.03.13.484154 (2022).
47. Jain, N., Iyer, K. V., Kumar, A. & Shivashankar, G. V. Cell geometric constraints induce modular gene-expression patterns via redistribution of HDAC3 regulated by actomyosin contractility. *Proceedings of the National Academy of Sciences* **110**, 11349–11354 (2013).